

INTERNATIONAL SOCIETY FOR SOIL MECHANICS AND GEOTECHNICAL ENGINEERING



This paper was downloaded from the Online Library of the International Society for Soil Mechanics and Geotechnical Engineering (ISSMGE). The library is available here:

<https://www.issmge.org/publications/online-library>

This is an open-access database that archives thousands of papers published under the Auspices of the ISSMGE and maintained by the Innovation and Development Committee of ISSMGE.

Investigations of Values of the Dynamic Penetration Resistance to Model Piles in Sand and Clay, Obtained from Tests

Essais sur les valeurs de la résistance à la pénétration dynamique rencontrée dans le sable et l'argile par des pieux modèles

by H. GRASSHOFF, Dr.-Ing., Bremen, Germany

Summary

The writer presents the results of tests in which rapidly moving model piles were photographed by a high-frequency slow-motion camera as they penetrated into sand. The curve of dynamic resistance was obtained from double graphical differentiation of the space-time diagrams obtained in the tests. The physical factors that influence the dynamic resistance are deduced on the basis of the conformity of the resistance diagrams to mathematical laws. The results are compared with those of similar tests carried out in clay and with the results of pile-driving tests in sand. The investigations are of interest in connection with the theory of dynamic pile-driving formulae and their practical applications.

In contrast to knowledge of the distribution of static forces in the subsoil, only little is known of the action of dynamic forces in the vicinity of rigid objects penetrating rapidly into soils. No basic formulae are available for the latter conditions. A knowledge of the dynamic forces in soils is of considerable importance in the theory of dynamic pile-driving formulae and their practical application.

Model tests have been carried out in 1944 by *Grasshoff* (1947) in the former Institute for Soil Mechanics and Foundation Engineering (Prof. Dr. *Loos*, Berlin). They are intended to be a preliminary contribution toward an understanding of basic problems concerning the action of dynamic forces in different types of soil. The purpose of the tests was to measure and to evaluate mathematically the variation in dynamic resistance to the penetration of rigid objects into sand. Since no previous test results were available, the tests were arranged to be of fundamental character and were carried out under somewhat simplified conditions. Bullet-shaped objects of various sizes (\varnothing 5, 7 and 9 cm), that might be likened to the tips of model piles, were projected into carefully prepared sand.

Sommaire

L'auteur présente, filmés au ralenti, les résultats d'essais sur des modèles de pieux pénétrant rapidement dans du sable. La courbe de résistance dynamique a été calculée à l'aide d'une double différenciation graphique des diagrammes espace-temps obtenus dans les essais. Les facteurs physiques qui influencent la résistance dynamique sont établis sur la base de la conformité du diagramme de résistance aux lois mathématiques. Les résultats sont comparés à ceux obtenus avec des essais similaires dans de l'argile et à des résultats d'essais de pénétration de pieux dans du sable. Ces recherches sont intéressantes, considérées en relation avec la théorie conduisant aux formules de fonçage dynamique et pour leur application dans la pratique.

The relative density and the water content of the sand were varied. Each test was photographed by means of a high-speed motion-picture camera (2500 frames per second). To permit photographing the projectiles during penetration, as well as to stabilize them, thin rod-shaped extensions were attached to the test objects. These rods protruded from the soil (Fig. 3). The positions of the projectiles determined from the slow-speed motion-picture film were closely and regularly spaced so as to provide a very exact time-penetration diagram. The relationship between the velocity and the penetration was obtained by one graphical differentiation of the time-penetration diagram, whereas the resistance curve was obtained by double differentiation. Fig. 1 shows the curves for time, velocity, and resistance as a function of the penetration, as obtained from the tests and derived by differentiation. Because of the inevitable inaccuracy in graphical differentiation the derived curves have only a qualitative value.

The resistance-penetration curves of the 40 individual tests which are of primary interest in this connection all show a sharp rise at the beginning of penetration up to a maximum

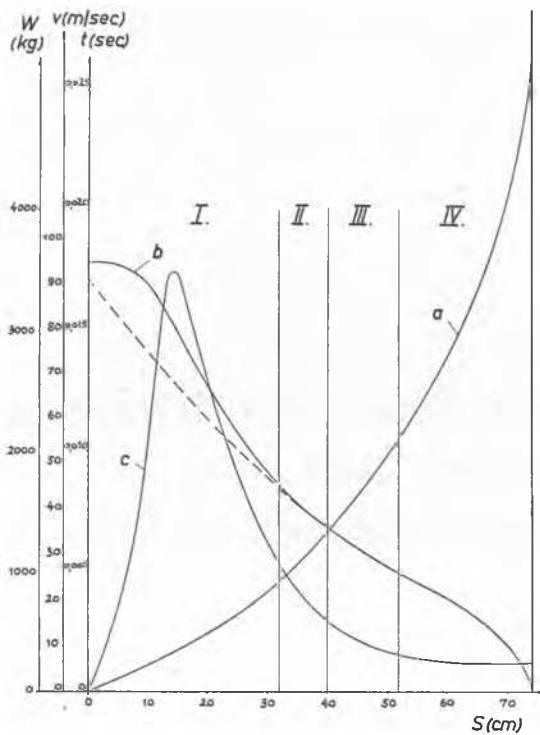


Fig. 1 Pile Driving Tests (according to *Grasshoff*), Sand, Test No. 12, Pile \varnothing 7 cm
 (a) Penetration-Time Diagram (Original Curve)
 (b) Velocity-Penetration Curve
 (c) Resistance-Penetration Curve
 (I) Zone of Impact
 (II) Resistance of Inertia Predominates (Logarithmical Curve)
 (III) Frictional Resistance Predominates (Straight Line)
 (IV) Static Resistance of Cohesion Predominates (Parabolic Curve)
 Essais avec pieux modèles (d'après *Grasshoff*), sable, essai n° 12, pieu \varnothing 7 cm
 a) Diagramme espace-temps (courbe originale)
 b) Courbe vitesse-espace
 c) Courbe résistance-espace
 I) Zone de choc
 II) Résistance d'inertie prédominante (courbe logarithmique)
 III) Résistance due au frottement prédominante (ligne droite)
 IV) Résistance statique due à la cohésion prédominante (courbe parabolique)

value of resistance. The resistance then drops almost as rapidly as it rose and continues to decline slowly (Fig. 1). The last section of the curve shows an almost constant curvature. When the model pile had come to rest, a more or less large static resistance still remained as a result of temporary elastic defor-

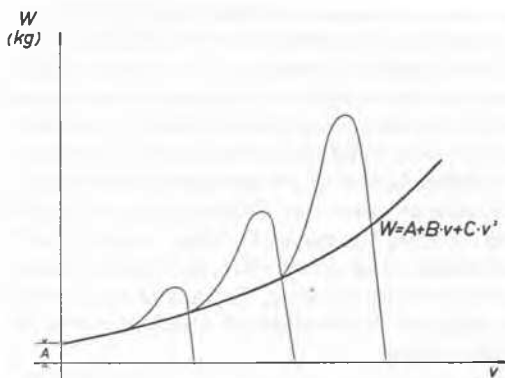


Fig. 2 Resistance-Velocity-Diagrams, Sand (according to *Grasshoff*)
 Diagrammes résistance-vitesse, sable (d'après *Grasshoff*)

mation of the sand. After a certain time and after relaxation of the stresses this resistance is likely to disappear.

The principle involved is illustrated by Fig. 2 which represents three resistance diagrams for similar model piles and similar sand, but different striking velocities. The curves are so arranged that the final points coincide where the model piles came to a stop. The diagram illustrates that the high value of the maximum resistance is evidently an impact effect. For equal velocities of the projectile, different resistance may develop depending upon whether the velocity is one at impact or one corresponding to the deceleration of an even higher impact velocity. The heavy curve in Fig. 2 may be considered as representing the dynamic resistance in relation to velocity if the influence of the striking impact is eliminated. This curve can be expressed tentatively by a trinomial geometrical progression:

$$W = A + Bv + Cv^2$$

The dimensions of the quantities in this expression indicate the physical properties of the sand to which the constants A , B and C correspond. The dynamic resistance W , and likewise the individual members of the geometric progression, are expressed in kg and are, therefore, forces. The constant A represents that part of the resistance independent of velocity, that is, the reaction caused by a static load. It depends on the arrangement of the grains of sand (friction at rest) and on the cohesion of the material. The static resistance may increase up to an ultimate value q_g . The structure of the soil will then break down and will yield suddenly and jerkily. According to other model tests (*Press*, 1939), q_g may be taken with sufficient accuracy as directly proportional to the cross-section of the penetrating projectile:

$$A \text{ (kg)} = FA' \text{ (cm}^2 \text{ kg/cm}^2 = \text{kg)}$$

Accordingly, the constant A' is expressed in kg/cm^2 . It corresponds to the ultimate resistance modified by a dimensionless shape factor. If the part of the resistance represented by the second member of the geometrical progression is first assumed

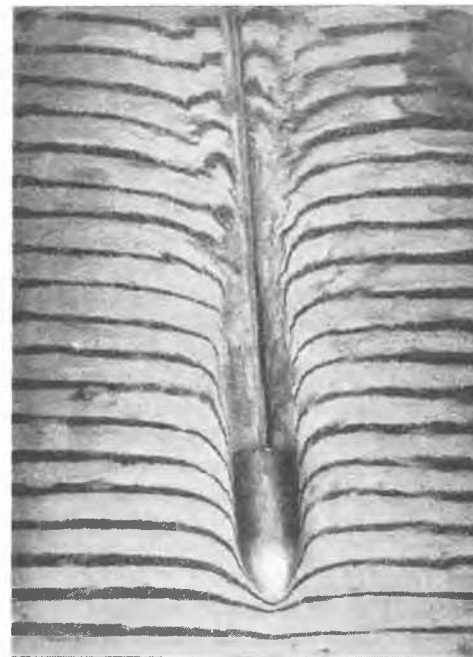


Fig. 3 Model-Pile Penetrating Into Sand (\varnothing 7 cm)
 Pieu modèle pénétrant dans du sable (\varnothing 7 cm)

to be proportional to a fixed linear dimension of the test body, such as, the perimeter U , the constant B' is measured in $\text{kg} \cdot \text{sec}/\text{m}^2$; thus B' represents the dynamic viscosity η :

$$Bv(\text{kg}) = UB'v(\text{m kg} \cdot \text{sec}/\text{m}^2 \cdot \text{m}/\text{sec} = \text{kg})$$

The viscosity is a physical property created in the vicinity of rigid objects penetrating into a liquid or soft medium even at slow velocities. On account of internal friction, moving

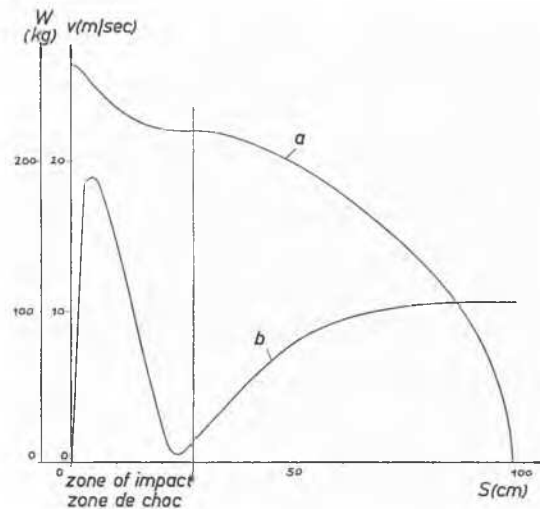


Fig. 4 Pile Driving Tests (according to *Zweck*), Clay, Test No. 126, Pile \varnothing 7 cm
 (a) Velocity-Penetration Curve
 (b) Resistance-Penetration Curve
 Essais avec pieux modèles (d'après *Zweck*), argile, essai n° 126, pieu \varnothing 7 cm
 (a) Courbe vitesse-espace
 (b) Courbe résistance-espace

friction and cohesion, a temporary velocity is imparted to adjacent particles of the medium at the circumference of the penetrating object. The velocity of the particles decreases more or less as the distance from the test body increases. Fig. 3 clearly shows this effect of the penetrating test body on the surrounding grains of sand. Evidently the sand behaves like a viscous liquid. The viscosity η is a function of the difference in velocity between adjacent particles within layers whose boundaries move parallel to each other in opposite directions. The viscosity is almost insignificant in water, but it increases to quite a high value in oil and plastic materials. Since sand possesses large internal friction, the property that might be likened to viscosity will in this case display even higher values. Although methods are known for the determination of the numerical value of viscosity for most liquids, none is known for quasi-liquid media such as sand. This may be explained by the fact that slippage in a single-grain structure is a complex phenomenon that takes place somewhat arbitrarily between the different grains within a space. Therefore, it is likely that the constant B' also includes a shape factor and a friction factor depending upon the surface of the test body.

The third member of the geometrical progression contains the square of the velocity. In accordance with the law of resistance to motion of rigid balls in liquids, e.g. as ascertained by *Bauer* (1926) for steel balls shot through water, this member represents that part of the resistance created by the inertia of the particles in the vicinity of the moving object. It is equal to the difference in pressure in front of and behind the object. According to the basic principles for liquids, this difference in

pressure for great velocities is approximately proportional to the square of the velocity. If we assume with *Bauer* that this resistance of acceleration is proportional to the cross-section of the penetrating test body, the constant C' has the dimension $\text{kg} \cdot \text{sec}^2/\text{m}^4$, that is of the density:

$$Cv^2(\text{kg}) = FC'v^2(\text{m}^2 \text{kg} \cdot \text{sec}^2/\text{m}^4 \cdot \text{m}^2/\text{sec}^2 = \text{kg})$$

The density (γ/g) is the direct cause of the acceleration resistance. It is also likely that the constant C' does not express the true density of the medium but also contains a factor related to the shape of the test body.

A remarkable feature of the curves obtained from these tests is the steep rise to a maximum value of resistance, forming a sort of steeple above the mathematical curve of the geometrical progression. This is obviously an impact phenomenon which is probably due to the initial inertia of the soil particles. In order to produce a region of dynamic forces which in a way can be compared to the flow of liquid (Fig. 3) and to start a wave of pressure which precedes and runs away from the point of the penetrating object, as in a solid body, a certain amount of energy is required. This is shown by the rather large size of the area beneath the steeple-like rise of the resistance curve.

The resistance-velocity curves (Fig. 2) show that, if the impact velocity decreases, this area does not decrease proportionally but rather more. In connection with pile driving, this would indicate that with increasing height of fall and correspondingly increasing energy, the falling ram loses energy not in proportion to the increased height but even to a greater extent. This fact explains the experience sometimes observed in pile driving that it is more economical to use smaller impulses and more blows per minute (for example in steam pile drivers) than larger and fewer impulses.

Test bodies projected into plastic clay under similar circumstances led to curves that differed greatly in the zone of impact from those derived from tests in sand (Fig. 4).¹⁾ On

¹⁾ Dr.-Ing. *Zweck*, who carried out numerous ramming tests in clay was kind enough to let the author have his data on this test. Other test data were unfortunately destroyed during the war.

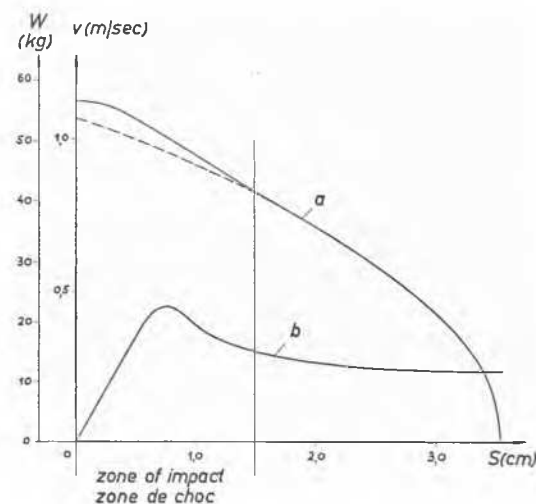


Fig. 5 Pile Driving Tests (according to *Hoffmann*), Sand, Test No. 21, Pile \varnothing 3.2 cm
 (a) Velocity-Penetration Curve
 (b) Resistance-Penetration Curve
 Essais avec pieux modèles (d'après *Hoffmann*), sable, essai n° 21, pieu \varnothing 3,2 cm
 (a) Courbe vitesse-espace
 (b) Courbe résistance-espace

the whole the values of resistance were smaller than in sand, as would be expected. After a steep rise to a maximum value the resistance drops almost as quickly to nearly zero and then gradually rises again to a constant value. This remarkable shape of the curve may be explained by the explosion-like phenomenon observed when the projectile strikes the clay and produces a hollow space. As long as the projectile moves in this cavity it meets practically no resistance. Resistance is met only when it has passed through this cleared space and again strikes the clay. These explosion-like displacement phenomena, however, are not encountered when piles are driven into clay because of the much smaller ramming impulses.

The author carried out the graphical differentiation of a time-penetration curve from *Hoffman's* ramming tests (*Hoffman*, 1943) with model piles in sand. This differentiation resulted in the velocity-penetration curve and in the resistance-penetration curve shown in Fig. 5. It is worth mentioning that here, too, the resistance curve shows a noticeable although small ascent at the beginning of penetration although the ramming energy is very small (1.65 m · kg).

The process of the penetration of rigid objects into homogeneous soils can be expressed as an equation of energy:

$$\frac{mv_0^2}{2} = \int_0^s W ds; \quad mvdv = Wds; \quad s = m \int_0^v \frac{v dv}{W} \quad (1)$$

m = mass of the test object (kg · sec²/m)

v = velocity of the test object (m/sec)

s = penetration distance of the test object (m)

W = function of dynamic resistance (kg)

A, B, C = constants of the function of dynamic resistance which include the physical properties of the penetrated medium.

If the individual members of the geometrical progression are substituted into the integral in different combinations the solution of the integral of equation (1) leads to the various characteristic velocity-space curves shown in Fig. 6. These mathematically derived curves naturally do not include the influence of the initial impact, which is marked by the steep-like rise of the resistance to a maximum. The various parts of resistance that predominated in the phenomena can be seen from that part of the velocity-space curve which is no longer affected by the initial impact. Like the nearly parabolic end of *Hoffman's* velocity-space curve (Fig. 5), this resistance in the case of a normal driving process consists mostly of a factor independent of velocity, except in the zone of impact.

These observations show that in connection with pile driving and similar processes in soil, we do not deal with a constant value of dynamic resistance. The resistance curve, especially the initial rise to a maximum, is influenced in different ways by the ramming impulse and the physical properties of the subsoil (mostly by the consistency, water content, and relative

density). No relationship which could be expressed by a mathematical function is apparent between the static resistance of the pile and the average value of the dynamic resistance. We may imagine, however, that in a relatively uniform soil an empirical relation could be determined as a so-called correction factor on the basis of driving tests followed by loading tests.

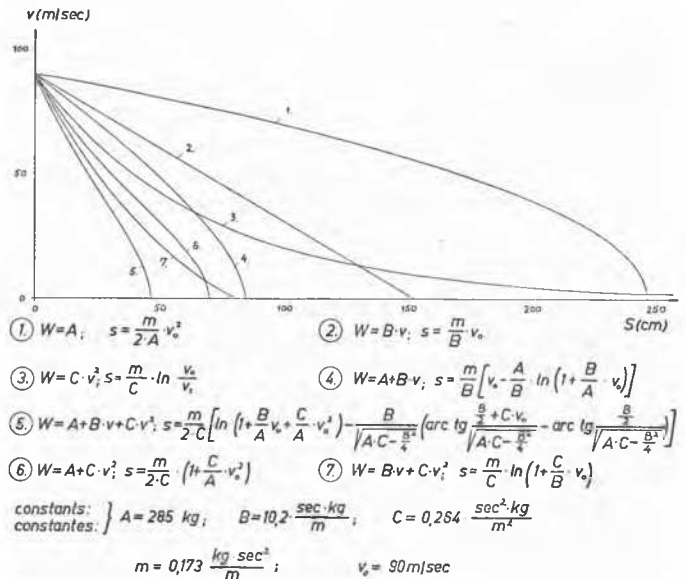


Fig. 6 Calculated Velocity-Penetration Curves for Various Laws of Resistance
Courbes vitesse-espaces calculées pour diverses lois de résistance

Schenck (1951) has already proposed this. The conditions required for these tests would be exactly the same as those for the driving of foundation piles. They should be carried out not only with the same piles and pile drives but also with exactly the same ramming impulses.

References

- Bauer, W.* (1926): Das Widerstandsgesetz schnell bewegter Kugeln in Wasser. *Annalen der Physik*, IV. Folge, Band 80, S. 232–244.
- Grasshoff, H.* (1947): Messungen des dynamischen Widerstandes an Modellpfählen in Sandböden und Untersuchungen über seine Gesetzmässigkeit. Dissertation Technische Hochschule Hannover, 1947.
- Hoffmann, R.* (1943): Der Rammschlag. In: *Forschungshefte aus dem Gebiete des Stahlbaues*, Heft 6, S. 55–61. Springer-Verlag, Berlin.
- Hoffmann, R.* (1948): Beitrag zur Frage der statischen und dynamischen Pfahltragfähigkeit. In: *Abhandlungen über Bodenmechanik und Grundbau*, S. 150–156. Erich Schmidt Verlag, Berlin-Bielefeld-Detmold.
- Press, H.* (1939): *Der Boden als Baugrund*. Verlag Wilhelm Ernst und Sohn, Berlin.
- Schenck, W.* (1951): *Der Rammfahl*. Verlag Wilhelm Ernst und Sohn, Berlin.